SIMULATION OF THE PERPENDICULAR RECORDING PROCESS INCLUDING IMAGE CHARGE EFFECTS

Martin F. Beusekamp and Jan H. Fluitman

Twente University of Technology, P.O. Box 217
7500 AE Enschede, The Netherlands.

Abstract - This paper presents a complete model for the perpendicular recording process in single-pole-head keeper-layer configurations. It includes the influence of the image-charge distributions in the head and the keeper layer. Based on calculations of magnetization distributions in stand-still situations, the model describes the relaxation process that takes place if the activated head is shifted along the recording layer, periodically switching its head field. The magnetization distributions thus derived are used in combination with a model for the readback process to calculate the readback flux and voltage pulses. For the sake of arithmetical convenience, the model was applied to a recording configuration with a thick single-pole head, but it can also be used for calculations with other head shapes, e.g. thin single-pole heads.

INTRODUCTION

The major advantage of perpendicular recording has always been considered to be the possibility of stable magnetization patterns with very high gradients (e.g. [1]). The question however, is not how sharp a transition could be, but how sharp it can actually be written by a given head. This problem can be investigated by a computer model which calculates the magnetization distribution development during the perpendicular recording process, with a head shifting along a recording layer, periodically switching its head field. The model is based on a previous one [2], with which it was shown that the influence of the image-charge distribution in the head and the keeper layer is significant. Therefore, in the present model the image-charge influence has also been taken into account.

The geometry of the investigated recording configuration is drawn in fig. 1, which shows the right-hand edge of a thick single-pole head (e.g. [3]) opposite a perpendicular recording layer with thickness t and separated from the main pole by an air gap g. The recording layer is backed by a keeper layer with an assumed $\mu=\infty$ and has an initial magnetization M_o in the direction as drawn. The recording layer material is assumed to have a rectangular (intrinsic) hysteresis loop with $M_s>H_c$ (fig. 2).

The model that will be described in this paper is not restricted to the given head geometry. The thick single pole was chosen for the sake of arithmetical convenience, but can be replaced by a pole with a different shape, e.g. a thin single-pole.

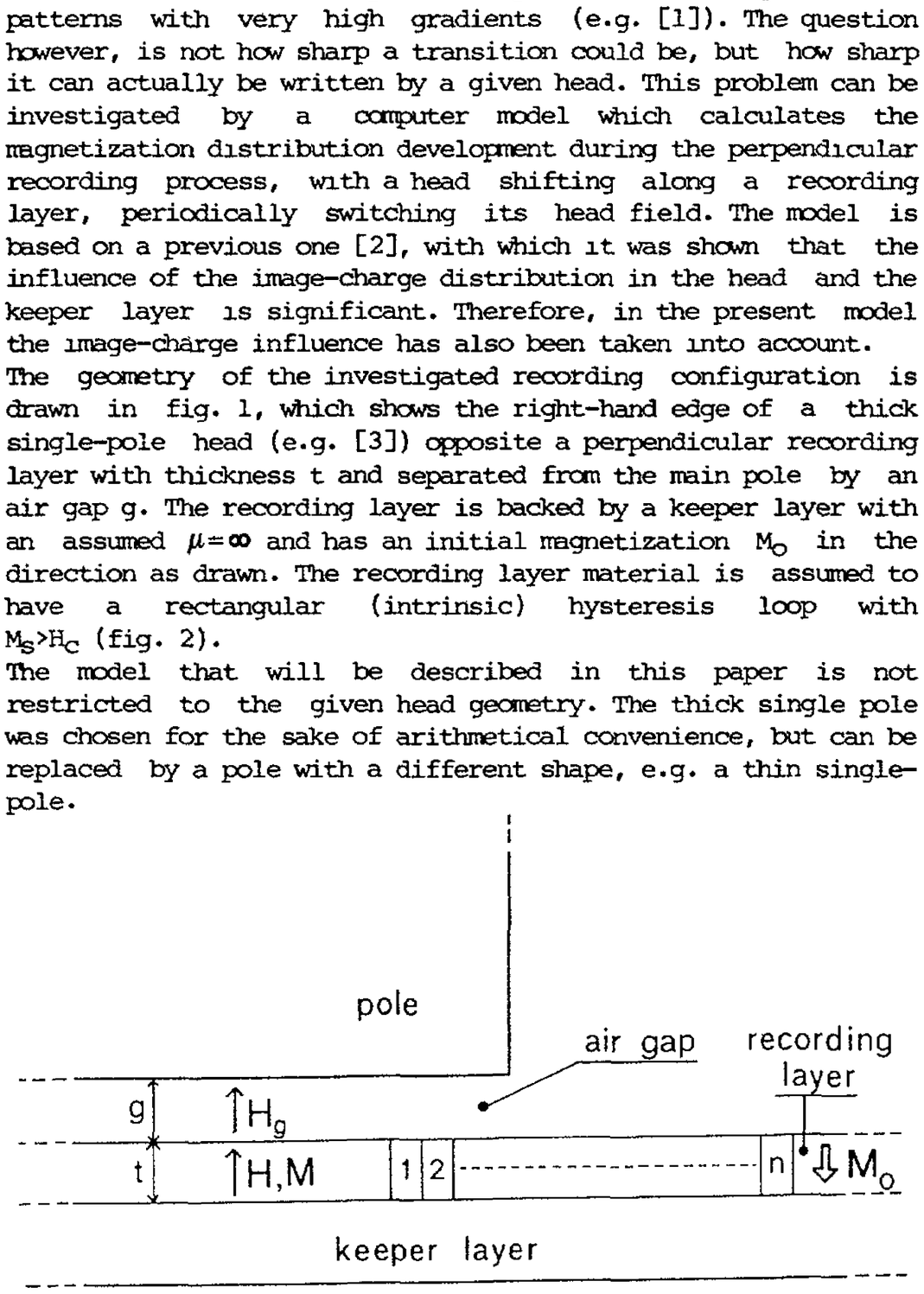

Figure 1. Geometry of pole-keeper head and recording layer.

STAND-STILL RECORDING

First, a situation will be considered in which the head is not moving with respect to the recording layer. In fig. 1, a head field with a direction opposite to M_o is switched on, thereby writing one transition near the edge of the head. During this writing, the magnetic field in every part of the recording layer will equal H_c, as has been shown by Wielinga et al. [4]. Based on this condition, an algorithm which calculates the magnetization distribution of the transition can be devised.

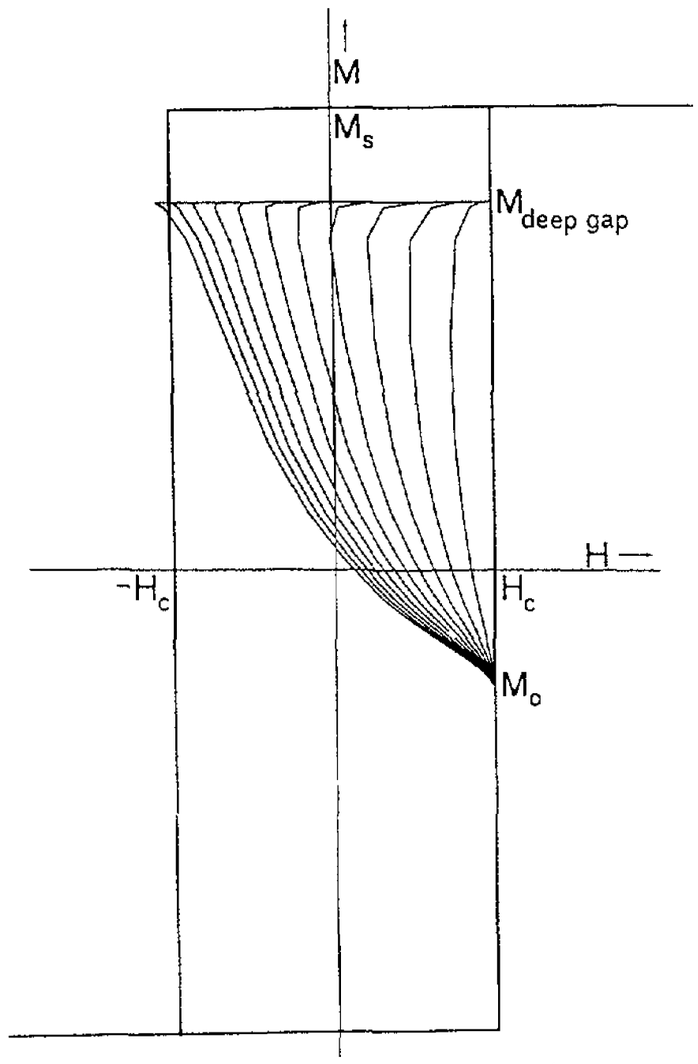

Figure 2. Hysteresis loop of the recording-layer material. The lines in the loop connect the MH-loci of all n stripes at a certain moment of the process. From right to left the first eleven steps of the relaxation process can be seen.

The recording layer region near the edge of the head is subdivided into n narrow stripes having magnetic fields H_j and magnetizations M_j ($1<=j<=n$), which are both assumed to be homogeneous throughout the j-th stripe. Only fields and magnetizations perpendicular to the plane of the recording layer are considered. We consider $H_1,\ldots,H_n$ and $M_1,\ldots,M_n$ as two n-dimensional vectors **H** and **M** respectively. The magnetic field in each stripe consists of three contributions: 1) the local head field H_h, 2) the contribution H_f of the recording layer regions outside the subdivided area, where the magnetization is assumed to be constant, and 3) the contribution H_m, caused by the magnetization in all n considered stripes. The vector H_m, consisting of the n values of H_m, can therefore be written as **[D].M**, where **[D]** is an n by n-matrix containing the magnetic interactions between each pair of stripes. The sum of the field contributions, which as stated must equal H_c in non-saturating recording, can now be written as:

$$H_h + H_f + [D].M = H_c \qquad (1)$$

where H_c is a vector containing n elements with a numerical value of H_c. Inverting **[D]** and rearranging the terms yields:

$$M = [D]^{-1}\ \{H_c - H_h - H_f\} \qquad (2)$$

The calculation of **[D]** and H_f can be done either with or without taking into account the fields caused by the image-charge distribution in the head and the keeper layer. In the latter case, **[D]** and H_f can easily be calculated with Coulomb's law for magnetic charges because the assumption of a homogeneous magnetization in each stripe implicates the concentration of magnetic charges in the top and bottom surfaces of the recording layer. In the case with the image charges taken into account, a conformal mapping method has to be used to calculate **[D]** and H_f [2]. The head field H_h can also be best derived numerically from a conformal mapping method; analytical approximations (Karlqvist [5], Szczech [6]) can, under extreme conditions, give rise to numerical

0018-9464/86/0900-0364$01.00©1986 IEEE

instabilities. The results of the stand-still calculations are given in fig. 3 for a characteristic case. Similar curves were discussed in [2].

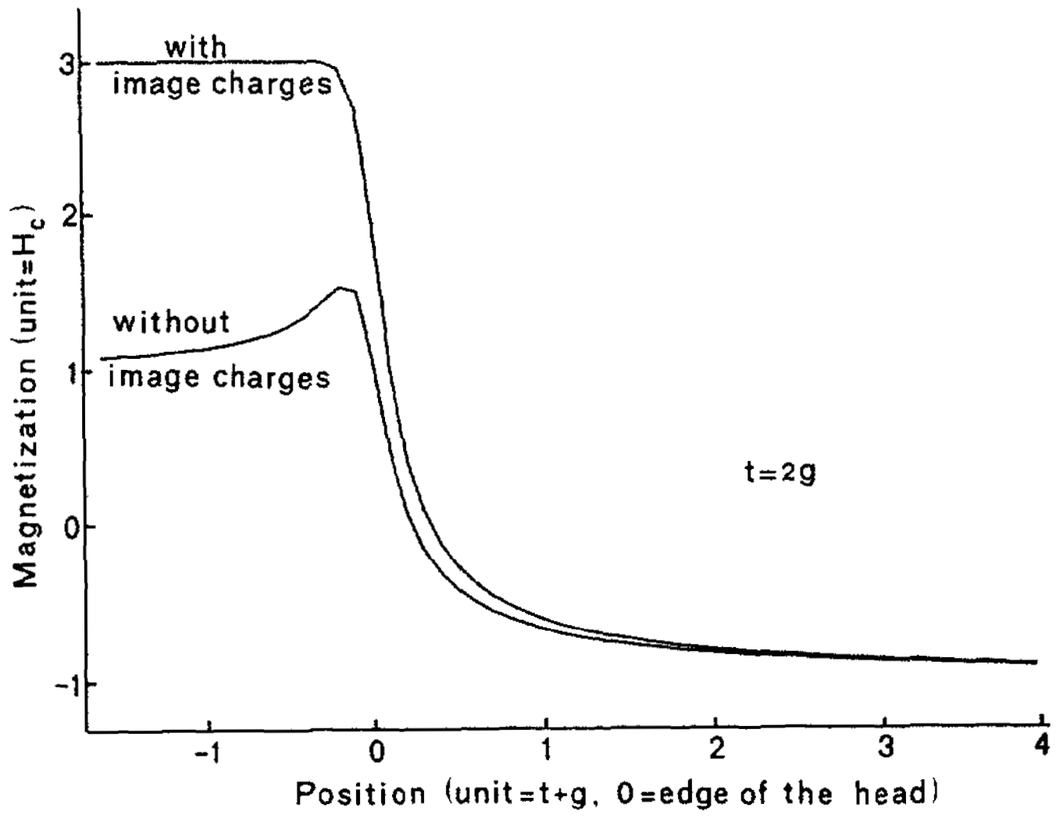

Figure 3. Comparison of transitions in the stand-still situation with and without image-charge influence being taken into account.

SHIFTING THE HEAD ALONG THE RECORDING LAYER

By shifting the activated head to the left, along the layer, the magnetic field in every part of the layer will decrease. Therefore, the assumption that $H=H_c$ throughout the layer will no longer hold, but because of the assumed rectangular minor hysteresis loops, the magnetization distribution does not change as long as $H>-H_c$ in every part of the layer. The loci, characterizing the M- and H-values in each of the n stripes will shift horizontally through the hysteresis loop along their own minor loops and at their own speeds, as illustrated in fig. 2, until a certain part of the recording layer reaches the left-hand side of the hysteresis loop. The magnetization in that part is then forced downwards along $H=-H_c$, initiating a relaxation process which will gradually spread out in the layer with every new locus that reaches $H=-H_c$.

Due to the discretization (fig. 1), the shift of the head along the layer can only be modelled in steps with a minimum width of one stripe. As previously mentioned, M_j will be constant as long as $H_j>-H_c$, so during this period the j-th stripe will cause a constant contribution to the field in the recording layer. As soon as H_j reaches $-H_c$ however, M_j will decrease, thereby decreasing the magnitude of its field contribution to all other stripes. Consequently, these will be retarded in their motion along M=constant or $H=-H_c$. This means, that if for instance the i-th stripe has reached the left-hand edge of the hysteresis loop after a given (mathematical) step in the model, it need not physically have done so. Other stripes may have reached the edge in an earlier stage of the displacement step, thereby retarding the i-th stripe sufficiently effectively to prevent it from reaching the edge. Therefore, special precautions in the relaxation algorithm have to be taken in order to correctly determine the sequence in which the loci reach $H=-H_c$, and check the mathematical solution after each displacement step for its physical correctness.

The relaxation process in the case in which the image charges are taken into account is illustrated by fig. 4, the upper contour of which is the result of the stand-still calculation. It can be seen how the typical self-magnetization peak develops, due to a strong demagnetizing effect between the edge of the head and the magnetization peak.

The inevitable presence of an image-charge distribution in the head and the keeper layer causes the case without the image charges being taken into account to be a purely imaginative one, to which the relaxation algorithm can not be applied. Nevertheless, to gain insight in the image-charge influence on isolated transitions, one would like to make a comparison between the two cases. In order to do so, we momentarily restrict ourselves to a deep-gap head field of $2H_c$. Without image charges taken into account, the sum of the head field and he demagnetizing field must equal H_c during stand-still writing. With a head field between 0 and $2H_c$, the demagnetizing field will vary between $-H_c$ and $+H_c$. Therefore, the transition as calculated in the stand-still situation without taking the image charges into account will not relax during the shift of the head. Figure 5 shows that the image-charge influence has led to isolated transitions that differ significantly.

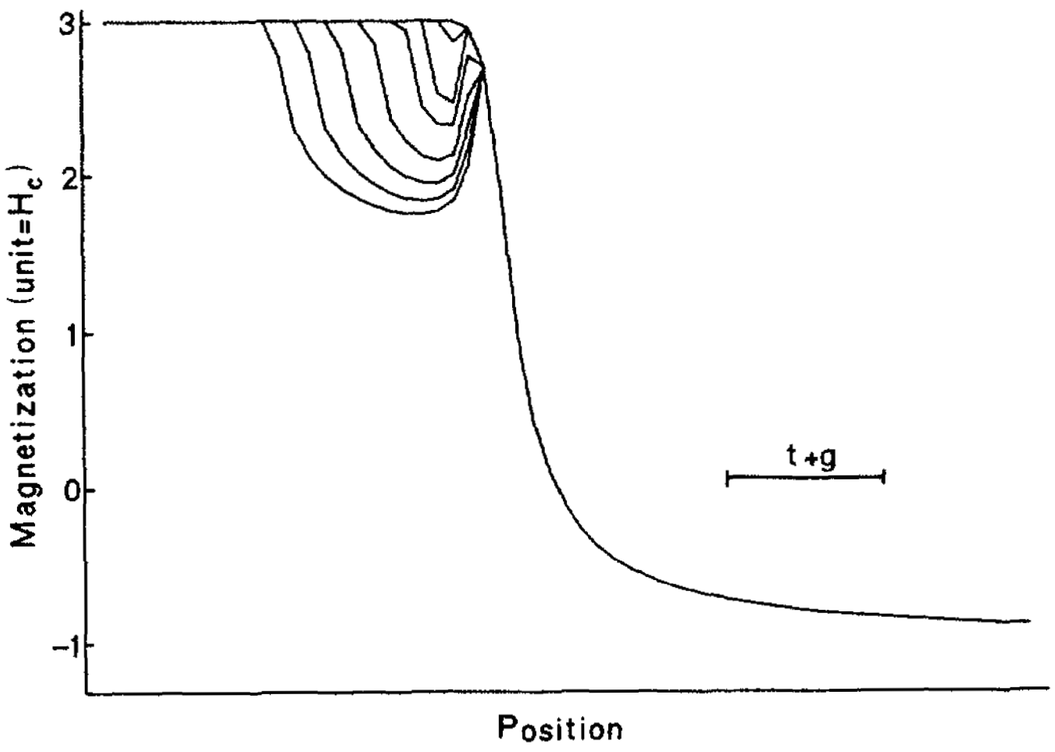

Figure 4. Development of the magnetization distribution during the shift of the head along the recording layer.

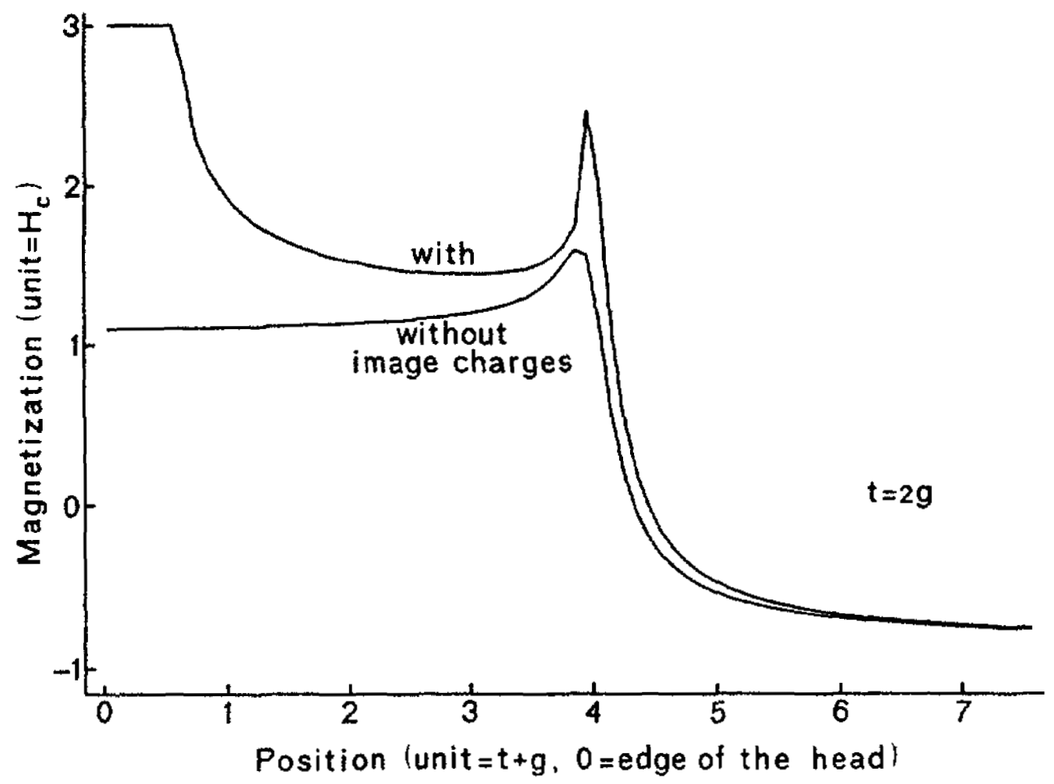

Figure 5. Comparison of isolated transitions calculated with and without taking the image-charge field into account.

SWITCHING THE HEAD FIELD

The ultimate aim of the simulation model is to calculate specified bit-patterns. Therefore, the influence of switching the head field while shifting the head along the layer was investigated. This switching is assumed to take place slow enough for the micromagnetic process to keep pace, but fast enough to neglect the displacement of the head during switching. As with shifting of the head, a switch of the head field from a positive value to a negative one will cause the total field in every part of the recording layer to decrease. It can therefore be modelled by an algorithm which closely resembles the one for the relaxation during shifting. This is illustrated by fig. 6, which shows that the magnetization under the head maintains its value during the first few steps of the switch, the field under the head thereby decreasing from $+H_c$ to $-H_c$. The magnetization under the head then rapidly changes to its opposite value, thereby affecting the level of the magnetization peak just outside the head.

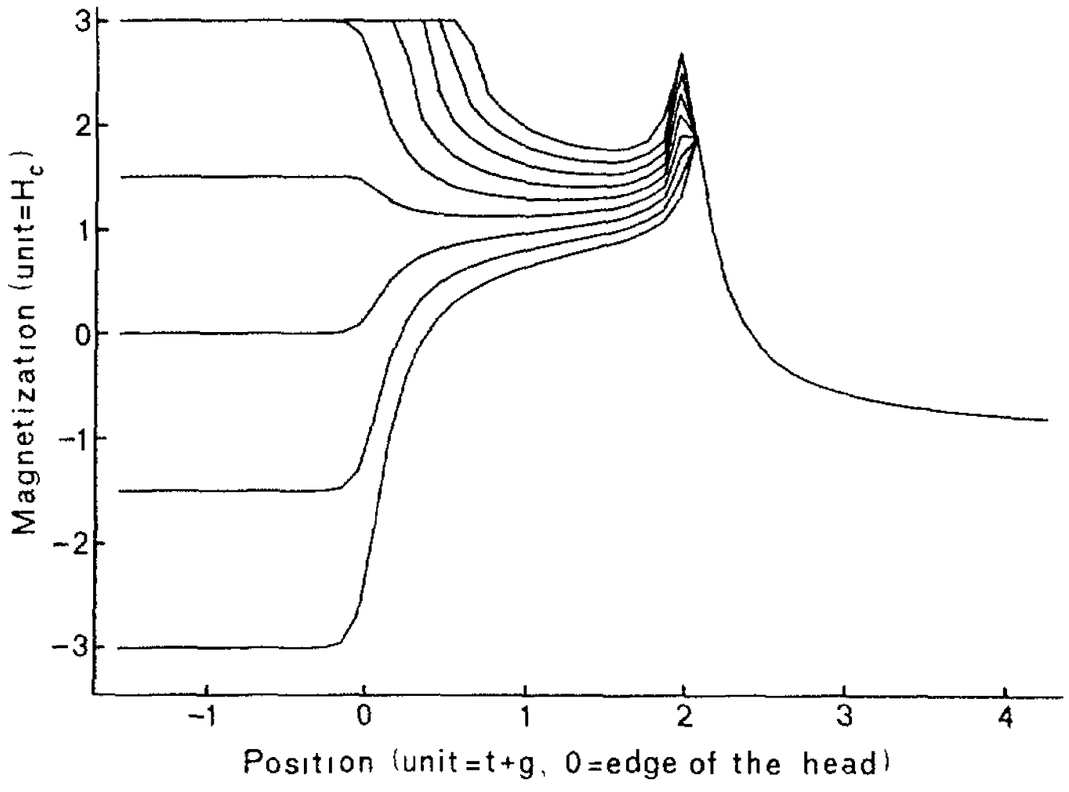

Figure 6. Development of the magnetization distribution during the switch of the head field from its original (positive) value to its opposite (negative) value, which was subdivided into eight equidistant steps.

We can now simulate the magnetization distribution caused by any input signal on the head, for instance a square wave (fig. 7). This figure also shows the effect of increasing the t/g-ratio, resulting in a sharper and higher magnetization pattern, as expected.
Parameter variation in the model showed that the magnetization peak after a head shift hardly depends on the maximum head field. It was already mentioned, that a head-field switch affects the height of the magnetization peak (fig. 6). This effect becomes more severe with a shorter distance between the edge of the head and the magnetization peak. This means that a higher bit-density will result in a magnetization pattern with lower peaks, contradicting wih the expectation that one might have, that a higher bit-density would cause a lower demagnetizing field and therefore a higher peak magnetization.

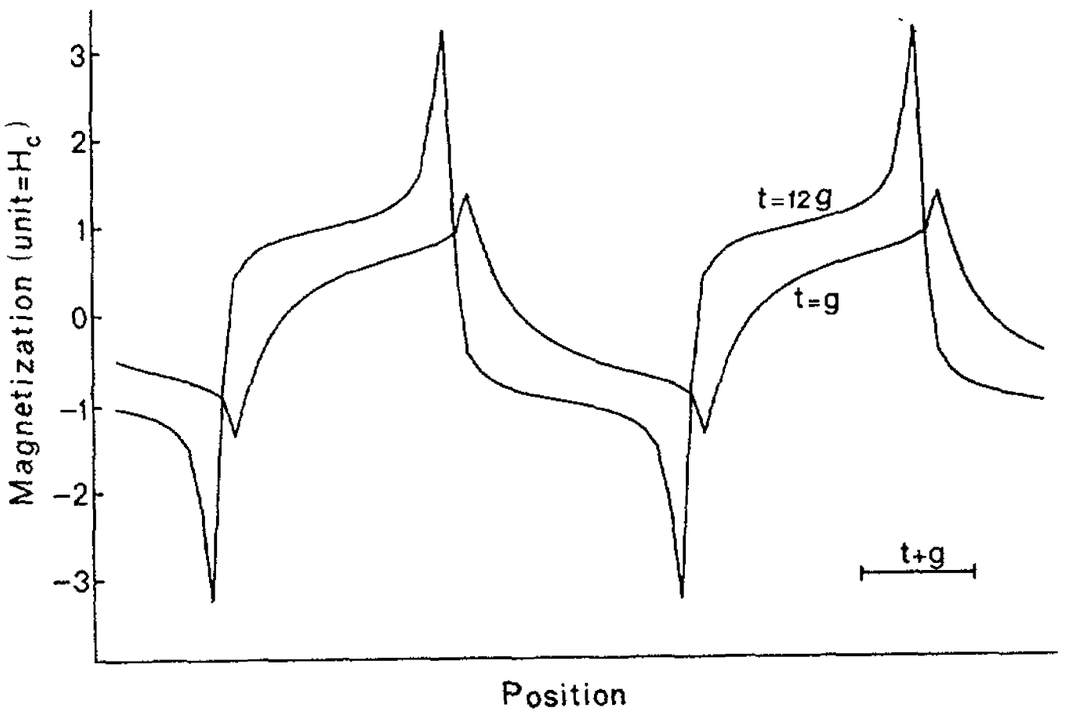

Figure 7. Comparison of magnetization distributions with equidistant transitions for t=g and t=12g respectively.

THE READ PROCESS

After calculating a magnetization distribution in the recording layer, the read process can be simulated by shifting the unactivated head along the layer again. This will obviously cause an image-charge distribution in the read head, which might affect the magnetization distribution to be read. Within the model's basic assumption of a rectangular hysteresis loop, there are two reasons why this effect will not occur. 1) The final magnetization value in each part of the recording layer is determined at the last moment at which the absolute value of the total field in that part equals H_c. Thereafter however, the relaxation process will continue to gradually cause the total field to decrease until the final value of the demagnetizing field in the situation of a completely removed write head is reached. Therefore, the demagnetizing field will generally be significantly smaller than H_c. 2) During writing, a semi-infinite part of the recording layer under the head is at a relatively high level of magnetization. This part has a great influence on the recording layer region just outside the head, where the final magnetization distribution is determined. However, this influence is absent during reading. These two reasons will generally prevent the absolute value of the total field in the recording layer from reaching H_c by the additional influence of the image-charge distribution in the read head. The readback flux can therefore be simply calculated from the correlation of the magnetization distribution and the head field [7]. Readback voltage can be obtained by differentiating the flux with respect to time, or, as the head velocity is assumed to be constant, with respect to the head position. Both flux and readback voltage are depicted in fig. 8 for a characteristic case. The assumed direction of motion of the read head will cause the steep trailing edges of the magnetization distribution (fig. 7) to be read before the leading ones, resulting in readback pulses with sharp leading edges.

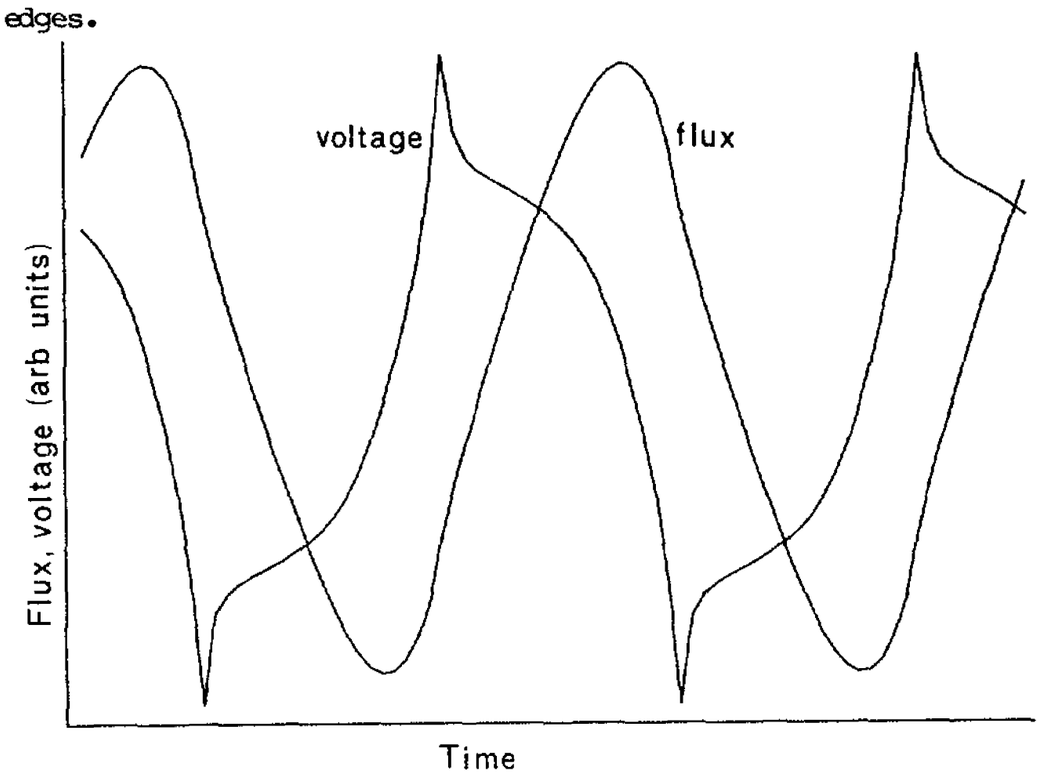

Figure 8. Readback flux and voltage (t=2g).

CONCLUSIONS

It can be concluded from the results of the given model for the perpendicular magnetic recording process, that, due to finite field gradients, transitions will always have a certain width. Their maximum gradient will mainly depend on the t/g-ratio. Peak magnetization will be lower with increasing bit density and, after a certain optimum, with increasing head field. Within the assumptions of the model, the positioning of a readback head will not affect the magnetization distribution in the recording layer.

REFERENCES

1) R.A. Johnson, C.S. Chi. "Fundamental Properties of Perpendicular Magnetic Recording." I.E.E.E. Trans. on Magn., Vol. MAG-17, No. 6, pp. 2544-6, November 1981.
2) M.F. Beusekamp, J.H. Fluitman. "Significance of Image-Charge Fields on the Write Performance of a Pole-Keeper Head." I.E.E.E. Trans. on Magn., Vol. MAG-21, No. 5, pp. 1414-6, September 1985.
3) A. Ohtsubo, Y. Satoh. "Thick Non-Parallel Single Pole Head for Perpendicular Recording from One Side." I.E.E.E. Trans. on Magn., Vol. MAG-18, No. 6, pp. 1173-5, November 1982.
4) T. Wielinga, J.H.J. Fluitman, J.C. Lodder. "Perpendicular Stand-Still Recording in CoCr-Films." I.E.E.E. Trans. on Magn., Vol. MAG-19, No. 2, pp. 94-104, March 1983.
5) O. Karlqvist. "Calculation of the Magnetic Field in the Ferromagnetic Layer of a Magnetic Drum." Trans. Royal Inst. of Techn. Stockholm, Vol. 86, pp. 1-27, 1954.
6) T.J. Szczech, D.M. Perry, K.E. Palmqvist. "Improved Field Equations for Ring Heads." I.E.E.E. Trans. on Magn., Vol. MAG-19, No. 5, pp. 1740-4, September 1983.
7) J.A. Geurst. "The Reciprocity Principle in the Theory of Magnetic Recording." Proceedings of the I.E.E.E., pp. 1573-7, November 1963.